ELSEVIER

Journal of Power Sources 100 (2001) 164–170

JOURNAL OF POWER SOURCES

www.elsevier.com/locate/jpowsour

New trends in electrochemical supercapacitors

C. Arbizzani[a], M. Mastragostino[b,*], F. Soavi[b]

[a]University of Bologna, Dipartimento di Chimica G. Ciamician, via Selmi 2, I-40126 Bologna, Italy
[b]University of Bologna, UCI-Scienze Chimiche, Radiochimiche e Metallurgiche, via S. Donato 15, I-40127 Bologna, Italy

Abstract

The present paper compares the performance of an n/p-type polymer supercapacitor based on n- and p-doped poly(3-methylthiophene) (pMeT) and of a hybrid supercapacitor, based on p-doped pMeT as positive electrode and activated carbon as negative, with that of a double-layer activated carbon supercapacitor (DLCSs), which is representative of the current state of supercapacitor technology. The data on the n/p-type supercapacitor demonstrate that this device is not fully competitive with the DLCSs because of its lower discharge capacity, although all the charge is delivered at high potentials and this makes it suitable for high-voltage applications. The data on the hybrid supercapacitor demonstrate that this device outperforms DLCSs, delivering higher average and maximum specific powers and significantly higher specific energy in the potential region above 1.0 V.

Keywords: Double-layer supercapacitor; Electrochemical supercapacitor; Hybrid supercapacitor; n-Doping; n/p-Type supercapacitor; Poly(3-methylthiophene)

1. Introduction

Supercapacitors can be used as uninterruptable power sources (UPSs), can be coupled with batteries to provide peak power and can replace batteries for memory back-up. The power requirements for a number of portable electronic devices have increased markedly in recent years and have exceeded the capability of conventional batteries to such an extent that great attention is being focused on electrochemical supercapacitors as energy storage systems, particularly on those in which high power density does not result from a reduction in energy density. The first part of this paper focuses on the present status of double-layer carbon supercapacitor (DLCS) technology and the second part deals with electronically conducting polymers (ECPs) as electrode materials in supercapacitors: the challenge is to come up with devices that outperform the DLCSs. The final section deals with a new supercapacitor type, a hybrid based on p-doped polymer as positive electrode and activated carbon as negative.

2. Experimental

The composite electrodes were prepared by mixing active material (pMeT or activated carbon), graphite (SFG44, Timcal) or acetylene black (AB, Hoechst), carboxy methyl cellulose (Cmc, Aldrich) and PTFE (Du Pont) to yield a paste. The paste was then laminated on the current collector (stainless steel grid, Delker) and dried at 80°C under vacuum over night. The composite carbon electrodes were based on 90% commercial activated carbon of high surface area, and the composite polymer electrodes were based on different percentages of pMeT (see Table 1), which was electrochemically synthesized under galvanostatic conditions at 10 mA cm^{-2} starting from 1.0 M 3-methylthiophene (Aldrich) in CH_3CN (Fluka) — 0.5 M Et_4NBF_4 (Fluka). The supercapacitors were assembled from two composite electrodes (Table 1) that were kept apart by a microporous PTFE separator and with propylene carbonate (PC, Fluka) — 1 M Et_4NBF_4 as electrolyte.

Impedance measurements of the supercapacitors and of each electrode were carried out in open circuit conditions in two- or three-electrode mode using a Solartron SI 1255 frequency response analyzer coupled with a 273 A PAR potentiostat/galvanostat. An ac amplitude of 5 mV was used and data were collected in the frequency range 100 kHz–10 mHz taking 10 points per decade. The cyclability performance of the supercapacitors was tested by repeated charge/discharge galvanostatic cycles at different current densities and cut-off potentials with a 273 A PAR potentiostat/galvanostat and a 545 AMEL galvanostat/electrometer. An Ag quasi-reference electrode, whose potential was checked versus SCE for each set of experiments, was used to monitor the electrode potentials during the charge/discharge

* Corresponding author. Tel.: +39-51-235-164; fax: +39-51-249-770.
E-mail address: mastrag@ciam.unibo.it (M. Mastragostino).

0378-7753/01/$ – see front matter
PII: S0378-7753(01)00892-8

Table 1
Electrode composition (% w/w) and the mass loading per cm^2 (weight of the current collectors not included) of total composite materials (m) and of the negative and positive electrode active materials, $m_{n,act}$ and $m_{p,act}$, respectively

Device code	m (mg cm^{-2})	$m_{n,act}$ (mg cm^{-2})	$m_{p,act}$ (mg cm^{-2})	Composition		Separator thickness (μm)
				Negative electrode	Positive electrode	
ACAC	20.0	9.0	9.0	Activated carbon, 90% SFG44, 5% Cmc–PTFE, 5%	Activated carbon, 90% SFG44, 5% Cmc–PTFE, 5%	50
PMPM	17.7	7.6	3.1	pMeT, 55% SFG44, 40% Cmc–PTFE, 5%	pMeT, 80% SFG44, 15% Cmc–PTFE, 5%	100
ACPM	19.0	6.5	9.4	Activated carbon, 90% SFG44, 5% Cmc–PTFE, 5%	pMeT, 80% AB, 15% Cmc–PTFE, 5%	50

cycles and during three-electrode mode impedance measurements. The electrochemical tests were performed at $T = 28 \pm 2°C$ in a MBraun Labmaster 150 dry box filled with argon. All chemicals were reagent-grade products, purified before use; the water content in the electrolyte solutions, which was checked with a Metrohm Karl-Fischer 684KF Coulometer before electrochemical tests, was in the 10–70 ppm range.

3. Results and discussion

3.1. Double-layer activated carbon supercapacitors

The supercapacitors on the market are DLCSs based on activated carbon of high specific area (1500–2400 $m^2\,g^{-1}$) with organic electrolytes; in such devices the energy is stored as charge separation at the carbon electrode/electrolyte interface. The surface area of activated carbons results from a complicated porous structure which involves pores of different size: macropores (>500 Å wide), mesopores (20–500 Å) and micropores (<20 Å). The smaller the pore size, the more difficult it is for the electrolyte to get in and, hence, the capacitance of these materials depends not only on the surface area but also on pore size distribution. At present, the best performing commercial activated carbons in organic electrolytes display capacitance values of about 120 $F\,g^{-1}$; these values are significantly lower than those in aqueous solutions because a large fraction of the carbon surface area is due to pores not accessible in organic electrolytes because of the larger dimension of the solvated ions.

We assembled and tested DLCSs in PC–Et_4NBF_4 by repeated galvanostatic charge–discharge cycles at different current densities (5, 10, 20 and 40 mA cm^{-2}) up to 10,000 cycles with cut-off potentials 0.0 and 2.8 V to estimate their performance in our experimental conditions as to discharge capacity, capacitance, specific energy and power and cycling stability. Figs. 1 and 2 and Table 2 display data of the ACAC supercapacitor, which has electrodes with the same composite mass loading per cm^2 (10 mg cm^{-2}) with 90% activated carbon (see Table 1 for electrode composition). Fig. 1 displays the discharge capacity, expressed in mAh g^{-1} of activated carbon, delivered with cycling at different current densities (the weight of the activated carbon of both electrodes was considered); the coulombic efficiency of each cycle was >99.9% as reported in Table 2, where the discharge capacity values expressed in C cm^{-2} are also reported.

These data demonstrate the high cycling stability of the DLCSs, which is strongly related to the high coulombic efficiency values. Fig. 2 shows the potential profile at 5 mA cm^{-2} of the ACAC supercapacitor, as well as those of each electrode, as an example. The potential profiles of the discharge curves of the supercapacitor were used to calculate the device capacitance, and these data at different cycle numbers and current densities are summarized in Table 2, where the capacitance values are reported in F cm^{-2} and F g^{-1} of the total active material. The maximum capacitance of the supercapacitor ACAC is 0.60 F cm^{-2} and

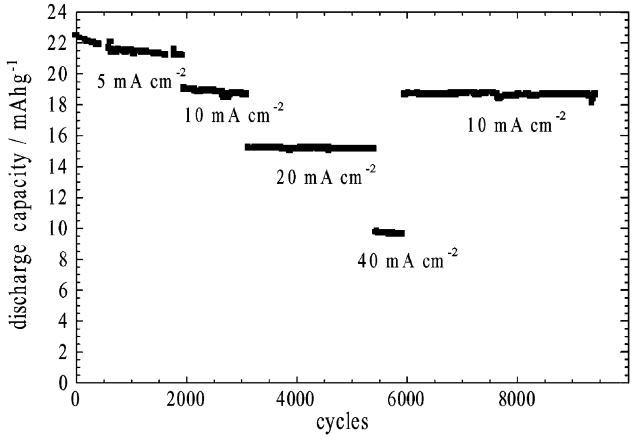

Fig. 1. Charge in mAh g^{-1} of total activated carbon (positive and negative electrodes) delivered by the ACAC device vs. cycle number at different current densities. Cut-off potentials 0.0–2.8 V.

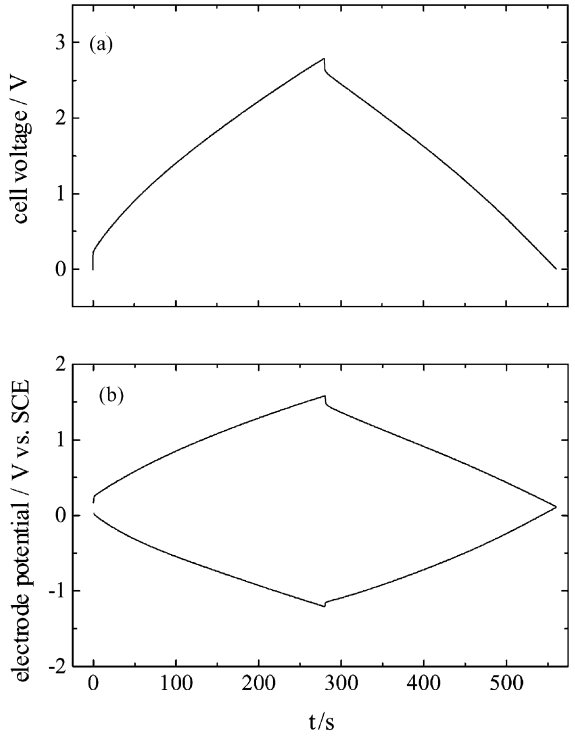

Fig. 2. Voltage profiles of (a) supercapacitor ACAC and of (b) its positive and negative electrodes at 5 mA cm^{-2}.

33 F g^{-1}, values that are representative of the state of DLCS technology; a value of 33 F g^{-1} for device capacitance, indeed, results from activated carbon electrodes of 132 F g^{-1} capacitance. We had already evaluated by impedance spectroscopy the equivalent series resistance (ESR) of DLCSs like the ACAC [1]. The value of ESR, which is mainly related to the charge process of the carbon electrodes, is higher than that of some commercial devices, scaled to 1 cm^2 of electrode area. However, it is known that activated carbons of high capacitance, such as the carbon of the ACAC supercapacitor, display a high resistance, a resistance which is due in part to reaching the pores of the smallest size and in part to charging them [2]. In effect, research in the DLCS field is mainly focused on the development of activated carbons with controlled pore size so as to favor larger micropores, to reduce their resistance and, thus, to improve supercapacitor-specific power despite material costs [3].

Table 2
Delivered charge (Q_d), coulombic efficiency (η (%)), supercapacitor capacitance ($C_{supercapacitor}$ in F cm^{-2} and F g^{-1} of total activated carbon of the positive and negative electrodes) from the galvanostatic cycles of the ACAC supercapacitor at different current densities[a]

Cycle number	i (mA cm^{-2})	Q_d (C cm^{-2})	η (%)	$C_{supercapacitor}$	
				F cm^{-2}	F g^{-1}
10–1930	5	1.41	100	0.60	33
1930–3080	10	1.24	100	0.56	31
3080–5410	20	1.00	99.9	0.50	28
5410–5920	40	0.64	100	0.43	24
5920–8000	10	1.23	100	0.55	30

[a] Cut-off potentials 0.0–2.8 V.

3.2. Polymer supercapacitors

Research is also investigating other classes of electrode materials such as ECPs, which show pseudocapacitive behavior, i.e. the energy storage in these materials is due to the Faradaic processes of p- and n-doping. The challenge is to come up with devices that outperform the specific power and energy of the DLCSs and that, even if charged and discharged by Faradaic processes, still present the same cycling stability.

ECPs are promising electrode materials for supercapacitors for three main reasons: (i) they are materials of high specific capacitance because the doping process involves the entire polymer mass; (ii) they are materials of high conductivity in the charged state; and (iii) their doping/undoping process is generally fast, so that devices with low ESR and high specific power are feasible; in addition, conventional ECPs are low-cost.

Fig. 3 compares the impedance spectra, recorded in three-electrode mode, of two composite electrodes with almost the same electrode active mass loading per cm^2 and organic electrolyte (PC–Et_4NBF_4): one is based on p-doped pMeT and the other on positively charged activated carbon. The composition of the two electrodes was 80% pMeT, 15% AB and 5% binder, and 90% activated carbon, 5% SFG44 and 5% binder, respectively. The figure highlights two key features of ECP electrode materials for coming up with

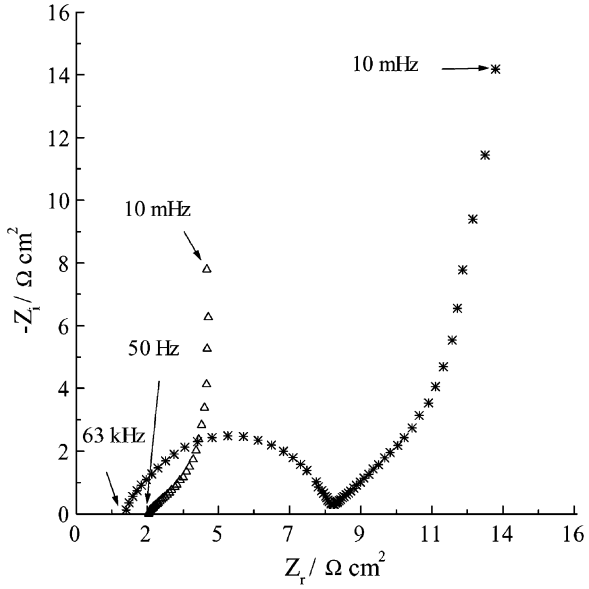

Fig. 3. Impedance spectra recorded in three-electrode mode of (✱) a positively charged composite electrode with 90% activated carbon (1.46 V vs. SCE, electrode active mass loading 9.1 mg cm^{-2}) and (△) a p-doped composite electrode with 80% pMeT (0.76 V vs. SCE, electrode active mass loading 9.3 mg cm^{-2}).

supercapacitors that outperform the DLCSs: the specific capacitance value of the p-doped polymer, 220 F g^{-1} (at 10 mHz), is significantly higher than that of the activated carbon, 120 F g^{-1} (at 10 mHz), and the resistance value for the charging process of the polymer electrode (2 Ω cm^2) is significantly lower than that for the activated carbon electrode (12 Ω cm^2).

The p-doping of ECPs has been extensively investigated and recently much attention has been devoted to the n-doping process with a view to polymer devices with an n-doped polymer as negative electrode and a p-doped one as positive (n/p-type supercapacitor). In fact, among the different polymer supercapacitor configurations proposed to date, the n/p-type is the device that can outperform the DLCS as all the doping charge is delivered during discharge at high potentials and both the electrodes are in the conducting (p- and n-doped) states.

In order to facilitate the n-doping process, many polythiophene derivatives have been developed, although the engineering of the thiophene unit to tune the potentials at which the doping processes occur leads to heavier molecules and also to higher materials cost. Polymers based on heavy thiophene derivatives require a higher injected charge than polythiophene to meet the criterion of high values of the specific parameters, and this can also adversely affect the polymer cycle life because of the greater mechanical stress on the materials.

Thus, for an n/p-type supercapacitor, we turned our attention back to a conventional thiophene-based polymer such as pMeT, which also has the advantage of low cost, and we demonstrated the high cycling stability for several thousands galvanostatic charge–discharge cycles of this n/p-type device using composite electrodes [4,5]. Although these results referred to devices which had not yet been optimized in terms of polymer content percentage in the composites, of electrode mass loading per cm^2 and of mass balancing between the two electrodes, we always achieved for the pMeT as positive electrode capacitance values per gram of pMeT double those for the pMeT as negative electrode, i.e. the p-doping/undoping process of pMeT yields capacitance values double those of the n-doping/undoping. Optimization of the electrode mass balancing must take into account these differences in capacitance, and a greater mass of pMeT per cm^2 has to be used for the negative electrode. For a proper comparison of the performance of the n/p-type pMeT-based supercapacitor with that of the double-layer supercapacitor ACAC, it is important that the total mass of the composite electrode materials is the same, i.e. ca. 20 mg cm^{-2} of device area. At present, the optimized mass content of pMeT in the composite electrodes is 80% for the positive and 55% for the negative electrode, and the calculation of electrode mass loading and balancing can be done as follows:

$$20 = \left(\frac{2x}{0.55}\right) + \left(\frac{x}{0.8}\right),$$

where x is the pMeT mass (in mg cm^{-2}) of the positive electrode.

Consequently, composite masses of the positive and negative electrodes of 5.1 and 14.9 mg cm^{-2}, i.e. 4.1 and 8.2 mg cm^{-2} of pMeT for the positive and negative electrodes, respectively, give a proper balancing of the two electrodes in terms of electrode capacitance per cm^2.

Given that the charge–discharge processes of ECPs are Faradaic and start at defined potentials, like the redox processes in batteries, and that the n-doping of pMeT starts at a very negative potential value, the excursion of potential of each electrode during charge should be ca. 0.5 V at maximum; this so as not to exceed the electrochemical stability window of the electrolyte during the charge of the negative electrode (n-doping of the pMeT). On the basis of these considerations and of capacitance values of 240 and 120 F g^{-1} of pMeT for the positive and the negative electrodes, respectively, we can estimate that the maximum cyclable charge per cm^2 by this n/p-type polymer supercapacitor assembled with electrodes balanced as above is 11 mAh g^{-1} of total pMeT (i.e. 6.8 mAh g^{-1} of total composite materials). The value of 11 mAh g^{-1}, which is limited by the potential excursion for the negative electrode, is significantly lower than that of the ACAC supercapacitor (22 mAh g^{-1}) with the same total composite mass (20 mg cm^{-2}). However, while the capacity of ACAC device was evaluated from the complete discharge down to 0 V, the charge delivered by the n/p-type pMeT-based supercapacitor will be released at high potentials, around 2.5 V, and this is a great advantage. In fact, it is known that for practical

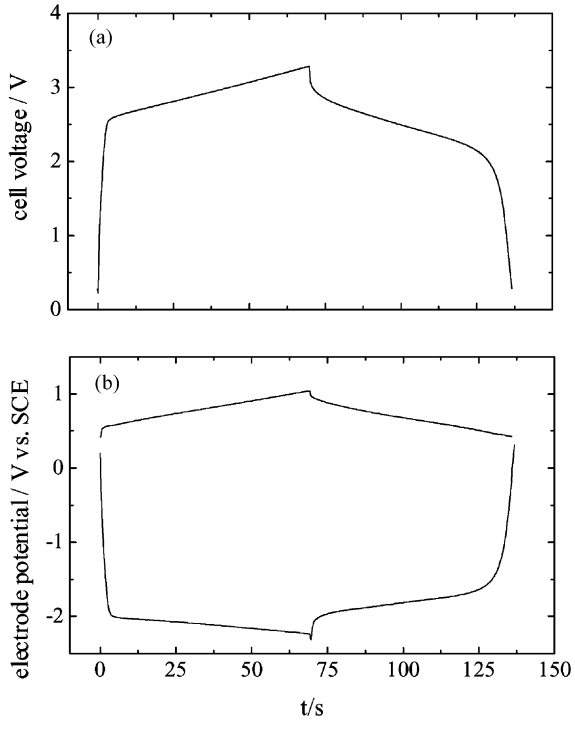

Fig. 4. Voltage profiles of (a) supercapacitor PMPM and of (b) its positive and negative electrodes at 5 mA cm^{-2}.

applications only the charge released at potentials higher than 1 V is appealing.

Fig. 4 shows the voltage profile at 5 mA cm^{-2} of the PMPM n/p-type pMeT-based supercapacitor and its electrodes, which were prepared with about the same mass loading and balancing as above (see Table 1 for electrode composition); the result in terms of the delivered charge, 9 mAh g^{-1} of total active materials, is as expected. Further investigation is in progress on this n/p -type pMeT-based supercapacitor, particularly on the increasing of the polymer percentage of the composite negative electrode and on the selection of the cut-off potential of the charge process, which is also related to device cycling stability.

3.3. Hybrid supercapacitors

Given that the capacitance and capacity of pMeT as positive electrode are sufficiently high for supercapacitor technology and the resistance to charging it is very low, we have developed a new type of supercapacitor, a hybrid device with p-doped pMeT as positive electrode and activated carbon as negative, whose charge and discharge processes are reported.

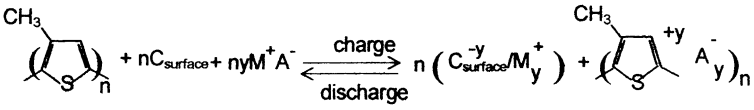

First, we demonstrated the cycling stability of this hybrid device by repeated galvanostatic cycles over 10,000 cycles in PC–Et_4NBF_4 at 20 mA cm^{-2} [1]. This was done on hybrid supercapacitors in which the active mass loading of the positive electrode was higher than that of the negative one, although the specific capacitance of pMeT as positive electrode is higher than that of the activated carbon. The estimation of the electrode mass loading and balancing is a more intricate matter for hybrid supercapacitors. While the ACAC double-layer supercapacitor was assembled with the same mass loading for both electrodes and the n/p-type pMeT-based supercapacitor assembled by taking into account the specific capacitance of the two electrodes, the balancing in hybrid supercapacitors must take into account both capacitances and different potential ranges for the charge processes of the two electrode materials. Since the Faradaic charge process of pMeT takes place in a potential range of ca. 0.5 V, a potential excursion of at least 2 V for the charge process of an activated carbon electrode that is capacitive in origin is required to reach potentials higher than 2.5 V for the charged supercapacitor. The hybrid supercapacitor was, thus, assembled with an active mass loading of the positive electrode higher than that of the negative.

Fig. 5 shows the voltage profile of the ACPM hybrid supercapacitor and of each electrode during a galvanostatic charge–discharge cycle at 5 mA cm^{-2} between 1 and 3.0 V. The percentage of active mass in the composites of the positive and negative electrodes was 80 and 90%, respectively (see Table 1 for electrode composition). The total mass of the two composite electrodes was 19 mg cm^{-2}, which is comparable with those of the ACAC and PMPM supercapacitors, and the ratio of the positive electrode active mass loading to the negative was 1.45. Table 3 shows device capacity (in C cm^{-2} and in mAh g^{-1} of total active materials), coulombic efficiency and capacitance (in F cm^{-2} and F g^{-1} of total active materials) evaluated from the discharge voltage profile of galvanostatic cycles of the ACPM device at different current densities. The comparison of the data in Table 3 with those in Fig. 1 shows that capacity values of the ACPM device are comparable to those of the ACACs. However, if we consider that the capacity values of the ACAC DLCS are related to discharge down to 0 V, as reported above, the ACPM supercapacitor outperforms the ACAC in terms of delivered charge at potentials higher than 1 V (19 and 15 mAh g^{-1} of active materials, respectively). In addition, note that at 5 mA cm^{-2}, the hybrid device capacitance is 0.62 F cm^{-2} and the capacitance per gram of total active materials is 39 F g^{-1}, while the capacitance of the ACAC was 0.60 F cm^{-2} and 33 F g^{-1}.

Fig. 6 shows the impedance spectra of a hybrid supercapacitor assembled like the ACPM, as described in the figure caption, and of its positive electrode; these spectra clearly indicate the low contribution of the polymer electrode to

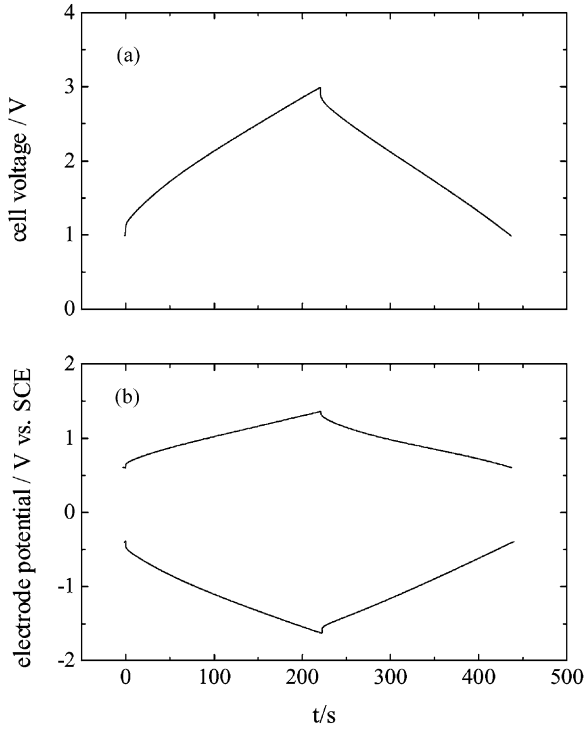

Fig. 5. Voltage profiles of (a) supercapacitor ACPM and of (b) its positive and negative electrodes at 5 mA cm^{-2}.

Table 3
Delivered charge (Q_d, expressed in C cm^{-2} and mAh g^{-1} of total active materials), coulombic efficiency (η (%)), supercapacitor capacitance ($C_{supercapacitor}$ in F cm^{-2} and F g^{-1} of total active materials) from the galvanostatic cycles of the ACPM supercapacitor at different current densities[a]

i (mA cm^{-2})	Q_d		η (%)	$C_{supercapacitor}$	
	C cm^{-2}	mAh g^{-1}		F cm^{-2}	F g^{-1}
5	1.08	18.8	99.0	0.62	39
10	0.96	16.8	99.5	0.59	37
20	0.77	13.4	99.7	0.55	35
30	0.60	10.5	100	0.50	31
40	0.46	8.1	100	0.45	28

[a] Cut-off potentials 1.0–3.0 V.

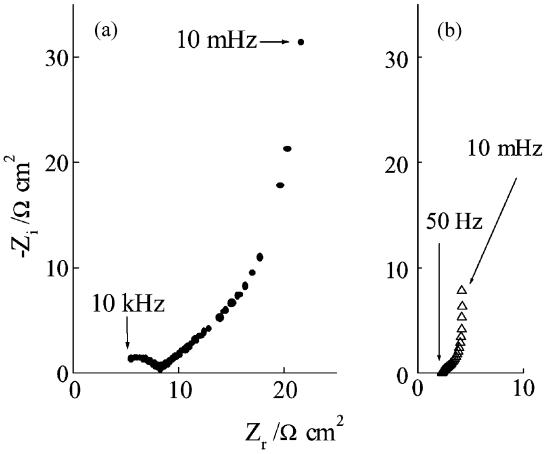

Fig. 6. Impedance spectra (10 mHz–10 kHz) of (a) charged hybrid supercapacitor in two-electrode mode and of its (b) positive electrode in three-electrode mode. The electrode compositions were: activated carbon 90%, SFG44 5%, Cmc–PTFE 5% ($m_{n,act}$ = 6.0 mg cm^{-2}) for the negative electrode and pMeT 80%, AB 15%, Cmc–PTFE 5% ($m_{p,act}$ = 9.3 mg cm^{-2}) for the positive electrode, and the total composite weight was 18.3 mg cm^{-2}.

device ESR. These results confirm our expectation that the hybrid supercapacitor strategy can give lower ESR than DLCS and, hence, higher specific power is expected.

The Ragone plot in Fig. 7 compares specific energy and average specific power performance of the ACPM hybrid supercapacitor with that of the ACAC double-layer carbon

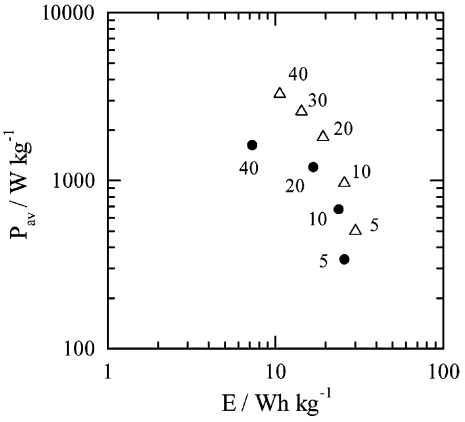

Fig. 7. Ragone plot for supercapacitors ACAC (●) (cut-off: 0.0–2.8 V) and ACPM (△) (cut-off: 1.0–3.0 V). Labels indicate the current density in mA cm^{-2}.

supercapacitor; both parameters were evaluated from the discharge curves of galvanostatic cycles at different current densities as

$$E = i \int \frac{V\,dt}{m}$$

$$P_{av} = \frac{E}{\Delta t_d},$$

where i is the current density, V the cell potential during discharge, m the total mass of the positive and negative composite electrodes per cm^2 (the current collectors not included) and Δt_d is the discharge time. This plot clearly demonstrates that the average specific power of hybrid supercapacitors is higher than that of the DLCSs of equivalent specific energy. Since, as noted above, working potentials above 1 V are required for practical applications, the performance of the two systems was more accurately compared by calculating the specific energy and average power delivered above 1 V, i.e. in the potential range 2.8–1.0 V, for the ACAC supercapacitor. The data at 5 and 20 mA cm^{-2} are reported in Table 4, which also includes the data of the Ragone plot. These results clearly show that the hybrid supercapacitor outperforms the double-layer supercapacitor not only in terms of power but also in terms of energy when

Table 4
Specific energy (E), average (P_{av}) and maximum (P_{max}) specific power of the ACPM hybrid supercapacitor and of the ACAC, evaluated at 5 and 20 mA cm^{-2}, at different cut-off potentials[a]

Supercapacitor	m (mg cm^{-2})	Cut-off (V)	i (mA cm^{-2})	E (Wh kg^{-1})	P_{av} (W kg^{-1})	P_{max} (kW kg^{-1})
ACPM	19	1.0–3.0	5	30	500	9
		1.0–3.0	20	19	1810	
ACAC	20	0.0–2.8	5	26	335	5
		0.0–2.8	20	17	1200	
		1.0–2.8	5	24	460	
		1.0–2.8	20	12.5	1570	

[a] Here m is the total mass of the two composite electrodes (weight of the current collectors not included).

the discharge is limited to 1 V, particularly at the higher current densities that are of main practical interest. The maximum specific power was also calculated for both types of supercapacitor:

$$P_{\max} = \frac{V_{\max}^2}{(4\mathrm{ESR} \cdot m)},$$

where the ESR values were estimated from one-half of the ohmic drop between charge and discharge curves of the galvanostatic cycles. These data, reported in Table 4, indicate that the replacement of an activated carbon electrode with a polymer-based one doubles the maximum specific power of the device.

4. Conclusions

The overall results for these tested supercapacitors, in which electrode mass loading is that required by cell scale-up, demonstrate that pMeT is a promising material for high power-and-energy devices. At present the results on pMeT n/p-type supercapacitors indicate that these devices are not fully competitive with DLCSs, especially as to the lower discharge capacity for which the negative electrode is mainly responsible. Nevertheless, for the high potentials at which the entire charge is delivered, n/p-type supercapacitors are worthy of further study, with improvements expected by increasing the polymer percentage of the composite negative electrode and by tuning the range in which the polymer (or polymers, in the case of asymmetric supercapacitors) is p- and, particularly, n-doped.

The results for hybrid supercapacitors based on pMeT as positive electrode and activated carbon as negative show that these devices outperform DLCSs, delivering higher average and maximum specific powers and, in the potential region above 1.0 V, significantly higher specific energy. Hence, these hybrid devices provide a positive response to the market demand for high power supercapacitors of high specific energy without significantly increasing costs. Indeed, the pMeT is a conventional ECP that can easily be prepared by chemical and electrochemical synthesis from a low cost monomer unit.

Acknowledgements

Project funded by European Commission within JOULE III (Contract no. JOE3-CT97-0047, SCOPE project) and by Progetto Finalizzato ''Materiali Speciali per Tecnologie Avanzate II'' (Contract no. 99.01.824.PF34). The authors wish to thank the partners in the SCOPE project CNAM (France), ENEA Department of Energy (Italy), Arcotronics Italia S.p.A. (Italy) and CEAC-Exide (France) for the contribution in the development of hybrid supercapacitors.

References

[1] A. Di Fabio, A. Giorgi, M. Mastragostino, F. Soavi, J. Electrochem. Soc. 148 (8) (2001) 4845.
[2] X. Andrieu, in: T. Osaka, M. Datta (Eds.), Energy Storage Systems for Electronics, Gordon and Breach, London, 2000, p. 521.
[3] A. Burke, J. Power Sources 91 (2000) 37.
[4] C. Arbizzani, M. Mastragostino, R. Paraventi, A. Zanelli, J. Electrochem. Soc. 147 (2000) 407.
[5] M. Mastragostino, R. Paraventi, A. Zanelli, J. Electrochem. Soc. 147 (2000) 3167.